Int. J. Heat Mass Transfer. Vol. 34, No. 2, pp. 415–425, 1991
Printed in Great Britain

0017–9310/91 $3.00 + 0.00

Model for contact heat transfer in mechanically stirred granular beds

KARUN MALHOTRA† and ARUN S. MUJUMDAR
Department of Chemical Engineering, McGill University, Montreal, Canada

(*Received* 22 *August* 1989 *and in final form* 26 *March* 1990)

Abstract—Although widely used in industry, design of mechanically stirred heated vessels is still an art. This research attempts, possibly for the first time, to evaluate surface-to-bed contact heat transfer rates for particulate beds stirred by paddle-type blades on the basis of a fundamental knowledge of the particle flow characteristics. A physical model for the wall-to-bed contact heat transfer coefficient based on particle renewal rates at the heated surface is presented. The particle renewal rates are estimated exclusively from measured information on particle movement in the vicinity of the heated vessel wall in a two-dimensional configuration. The heat transfer model includes the effects of agitator rotational speed, wall-to-blade clearance size, solids flowability and aeration.

INTRODUCTION

IN AN indirectly-heated vessel for granular solids, agitation improves heat and mass transfer rates via enhanced particulate mixing and high rates of particle renewal at the heated surface [1–3]. In such vessels, heat is supplied through the vessel wall, immersed heating elements or the agitator surface. Additional heat is frequently provided by direct contact with a gas as the heating medium, which may also be used to remove vapours in a drying operation. Besides being thermally efficient, other advantages of indirectly heated vessels include: minimal product contamination and degradation, generally lower capital and operating expenses, and easy operation under vacuum and controlled atmospheres. Such vessels can also effectively utilize a number of energy sources such as steam, hot purge gases, heat transfer fluids, etc. Difficulties in design, fabrication and maintenance are some drawbacks of these vessels used for thermal processing of particles. Also, in some industrial drying operations high degrees of dryness may be difficult to achieve.

Indirectly heated agitated vessels are widely used as dryers, heat exchangers and calciners. An industrial paddle-type stirred vessel is typically a long horizontal cylindrical trough with flat rectangular cross-sectioned blades mounted along the central agitator shaft. The equipment assembly may be slightly inclined horizontally to facilitate conveyance of solids along the trough. In case of indirect heating, heat is supplied through the walls and sometimes through the hollow agitator shaft and the blades. Such equipment finds wide ranging applications in industries processing products such as minerals and ores, chemicals, pharmaceuticals, polymers and food [2–4].

The advantages of stirred vessels include their ability to handle materials of different shapes, sizes and properties, easy control and very large hold-ups (up to 100%). Further, they can be easily employed in 'through-air flow' mode, leading to significant reduction in torque required for agitation [4] at modest air flow rates (less than the air flow rate required for minimum fluidization of the particles). The gas distributor and agitator are easily replaceable. Possible attrition and breakage of friable materials and relatively high maintenance costs are some of its disadvantages.

Particle mixing and flow patterns are important mechanisms governing the wall-to-bed contact heat transfer rates in mechanically agitated vessels [1, 5–8]. However, studies attempting to relate contact heat transfer to particle flow are scarce. Proper selection, design and scale-up of mechanically stirred heated vessels handling granular solids therefore requires an understanding of the flow dynamics of the solids within the bulk and the immediate vicinity of the heated surface. Particle flow and mixing characteristics of granular beds stirred by paddle-type blades are discussed in refs. [9–11]. In another publication the technique for estimating particle renewal rates along the heated wall in a stirred vessel is discussed based on the particle flow information [12]. This paper discusses the estimation of the particle–surface contact time (and subsequently contact heat transfer coefficient) from the particle renewal rates along the wall. A physical model based on the flow dynamics of solids and incorporating the effects of solids flowability, wall-to-blade clearance size and aeration is presented.

EXPERIMENTAL APPARATUS

The experimental set-up consisted of a horizontal nominally two-dimensional cylindrical vessel stirred by paddle-type blades and driven via a flexible coupling connecting the agitator shaft to the drive. The

† Present address: Murata Manufacturing Co. Ltd, Nagaoka-Shi, Kyoto 617, Japan.

NOMENCLATURE

B	blade height [m]
C	modified bulk compressibility of solids [—]
C_b	specific heat of granular bed [J kg^{-1} K^{-1}]
D	vessel diameter [m]
d_p	characteristic particle dimension [mm]
$E(t)$	expected value of particle–surface contact time (equation (16)) [—]
F	fraction of vessel circumferential area covered with particles [—]
H	average bed height at central midplane [m]
h	local wall-to-bed contact heat transfer coefficient [W m^{-2} K^{-1}]
h_{av}	overall wall-to-bed contact heat transfer coefficient [W m^{-2} K^{-1}]
h_c	packed bed heat transfer coefficient [W m^{-2} K^{-1}]
h_{ci}	instantaneous particle convective heat transfer coefficient [W m^{-2} K^{-1}]
h_c	overall particle convective heat transfer coefficient [W m^{-2} K^{-1}]
h_g	gas convective heat transfer coefficient [W m^{-2} K^{-1}]
h_r	radiative heat transfer coefficient [W m^{-2} K^{-1}]
h_s	wall-to-first particle layer heat transfer coefficient [W m^{-2} K^{-1}]
k_e	effective bed thermal conductivity [W m^{-1} K^{-1}]
k_f	fluid thermal conductivity [W m^{-1} K^{-1}]
L	circumferential length of particle covered surface area [m]
l	linear separation between two adjacent b1 blades [m]
N	agitator rotational speed [rev min^{-1}]
N_B	number of passes of blade b1 required by a particle to travel the distance from $0.1L$ to L [—]
N_b	number of passes of blade b1 required by a particle along the wall to traverse the distance L [—]
N_b^*	number of passes of blade b1 required to transport a particle along the wall just downstream of the grid up to $x = L$ [—]
Nu_{av}	average Nusselt number, $h_{av}d_p k_f^{-1}$ [—]
n	number of blades (b1) mounted on the shaft in the same axial and radial planes [—]
s_r	average size of surface asperities on contacting surfaces [m]
t	particle–surface contact time [s]
t_{av}	average particle–surface contact time [s]
t_R	time taken for the blade to travel length L [s]
Δt	time taken per pass of blade b1 [s]
ΔT	average wall-to-bed temperature gradient [K]
U	superficial air velocity through the bed [m s^{-1}]
U_{mf}	minimum fluidization velocity [m s^{-1}]
$V(x)$	particle velocity along the wall relative to the blade [m s^{-1}]
V_{bw}	linear velocity of blade extrapolated to vessel wall [m s^{-1}]
V_p	average particle velocity along the wall [m s^{-1}]
$V_{pi}(x)$	local particle velocity along the wall [m s^{-1}]
x	instantaneous particle position along the wall [m]
Δx	average particle displacement per blade pass along the wall [m].

Greek symbols

δ	thickness of the wall-to-blade clearance region [mm]
η_{av}	average efficiency of particle renewal along the vessel wall [—]
η_0	local efficiency of particle renewal [—]
η_R	$1-\eta_0$ [—]
Π	region of influence of the moving blade [m]
ρ_b	bulk density of the granular bed [kg m^{-3}]
ω	angular velocity of blade rotation [rad s^{-1}].

drive consisted of two belt-driven pulleys connected to a 3.7 kW variable speed d.c. motor. The motor speed could be controlled between 0 and 100 rev min^{-1}. Further details of the experimental set-up are available in refs. [9, 10].

Two horizontal cylindrical vessels of diameter 0.5 and 0.25 m and axial depths of 0.1 and 0.15 m, respectively, were employed for the particle flow experiments. The smaller vessel was constructed to allow experiments with aeration as well and was used for heat transfer experiments. It consisted of a perforated grid with an open area of 16% (1.6 mm holes on a 3.8 mm triangular pitch), and circumferential length 0.125 m. A conical hood at the top housed the air filter and was connected to a calibrated dry gas flow meter to monitor the air flow rate. The plenum chamber was filled with spherical glass beads to dampen turbulence in the air flow.

The wall-to-blade clearance region (in this study defined as the annular zone in the bed between the

Table 1. Range of operating parameters

Agitator rotational speed (N): 2–60 rev min^{-1}
Superficial air velocity through the bed (U): 0–50 m s^{-1}
U/U_{mf}: 0–0.6
Bed-to-blade height ratio (H/B): 3–6.5
Blade height (B): 0.025 and 0.05 m
Vessel diameter (D): 0.25 and 0.5 m
Wall-to-blade clearance size (δ): 2.3–37 mm

cylindrical vessel wall and the surface swept by the outer tip of the rotating blade) was varied between 2.3 and 37 mm. The range of the operating parameters and the thermophysical properties of the granular bed and particles are listed in Tables 1 and 2, respectively. Note that agricultural materials—rice, millet and linseed—were employed as model particles because of the diversity in their shape and surface characteristics. All the particles were screened to obtain an almost mono-dispersed size distribution.

RESULTS AND DISCUSSIONS

Heat transfer mechanism

The wall-to-bed contact heat transfer in moving, fluidized or agitated granular beds consists of three parallel mechanisms [1, 13]: particle convection, gas convection and radiation

$$h = h_c + h_g + h_r. \quad (1)$$

The particle convective, gas convective and radiative heat transfer coefficients are denoted by h_c, h_g and h_r, respectively.

Particle convection refers to the mechanism of energy transfer through the moving particles. Heat is transferred to a particle during its contact with the heated surface primarily by conduction through the gaseous gap in the vicinity of the contact point thereby increasing its internal energy. By random motion of the particles that surplus of internal energy is conveyed to and dissipated within the bulk of the bed. The most important parameter in evaluation of h_c is the particle–surface contact time. The particle–surface contact time varies greatly depending upon the nature of particulate flow in the granular bed (i.e. moving, fluidized, vibrated, stirred, etc.).

The gas convective heat transfer coefficient is insignificant (compared to h_c) at air flow rates used in this study (i.e. $U/U_{mf} \leqslant 0.6$). The radiative component of heat transfer becomes important only at higher bed temperatures (>800 K). Therefore, h_g and h_r are neglected in this study.

The particle convective heat transfer may be estimated from the following three heat transfer resistances in series [13, 14]:

(a) wall-to-first particle layer thermal contact resistance;

(b) resistance due to heat conduction in packed beds;

(c) resistance due to heat convection by particle motion.

The subject of wall-to-first particle layer heat transfer has been debated extensively [14–17]. Although it is generally agreed upon that there exists a conduction resistance ($1/h_s$) through the fluid between the surface and the contacting layer of particles, its formulation is still controversial. A review on the above subject is available in Gloski *et al.* [17] and Lybaert [18]. Recently an extension was proposed [19] of the wall-to-first particle layer heat transfer model of Schlunder [14], by incorporating the effects of particle shape and orientation at the contacting surface.

Heat conduction in packed beds is estimated from the 'packet renewal model' [20], assuming the granular bed to be a continuum in the vicinity of the heating surface (i.e. beyond the first particle layer). The instantaneous conduction heat transfer coefficient (h_c) was evaluated for a given particle–surface contact time under various boundary conditions. For an isothermal heat transfer surface, h_c is given as

$$h_c = \left\{\frac{k_e C_b \rho_b}{\pi t}\right\}^{1/2}. \quad (2)$$

Table 2. Thermophysical characteristics of the model particles

	Glass	Millet	Rice	Linseed
Actual size of particles (mm)	0.46 0.77	2.62 × 1.88	6.70 × 1.70	4.70 × 2.26 × 1.05
Characteristic length (mm)	0.46 0.77	1.88	1.70	1.05
Equivalent diameter† (mm)	0.46 0.77	1.89	2.50	1.82
Sphericity	1	0.99	0.815	0.805
Particle density (kg m^{-3})	2480	1090	1386	1078
Bulk density (kg m^{-3})	1500	675	815	655
Shape	sphere	ellipsoid	ellipsoid	flat disc
Surface	smooth	smooth	rough	smooth
Modified bulk compressibility	0.07	0.08	0.12	0.11
Specific heat of particle (J kg^{-1} K^{-1})	753	1600	1500	1380

† Based on a sphere of same volume as the particle.

For a constant heat flux boundary

$$h_c = \left\{\frac{k_e C_b \rho_b \pi}{4t}\right\}^{1/2}. \quad (3)$$

The thermophysical properties correspond to the 'effective' value of the granular medium within the heat penetration depth from the heat transfer surface.

Heat convection by particle motion is the least understood of the three heat transfer mechanisms. Martin [21] has summarized some of the features of this topic. Knowledge of particle motion and thermal gradients within the granular bed is necessary to evaluate its contribution to the overall contact heat transfer. In this study the number of particle-to-particle collisions were limited due to the intermittent nature of particle motion. Furthermore, the net displacements of the majority of the particles after each blade pass were confined to within a circular region of radius $1–1.5B$ [9, 10]. The thermal gradients in such localized regions are expected to be low (<0.5 K) for the ΔT values obtained in this study (typically between 5 and 15 K). Therefore, the resistance due to particle-to-particle convective heat transfer towards the wall-to-bed contact heat transfer may be neglected. Other authors [14, 22, 23] have made similar assumptions by qualitatively considering the granular bed to be thermally well mixed.

The particle convective heat transfer can then be written as

$$\frac{1}{h_{ei}} = \frac{1}{h_s} + \frac{1}{h_c} \quad (4)$$

where h_{ei} is the instantaneous overall particle convective heat transfer coefficient. Note that, for very short contact times ($t \to 0$), particle convective heat transfer is controlled by fluid conduction within the roughness asperities of the contacting surfaces ($h_{ei} \to h_s$). For 'large' contact times, $h_{ei} \to h_c$, i.e. it is a function of the thermophysical properties of the granular bed.

The time averaged overall particle convective heat transfer coefficient (h_c) is evaluated as

$$h_c = \frac{1}{t}\int_0^t h_{ei}\, dt. \quad (5)$$

Further, since $h \approx h_c$ (h_g and $h_r \to 0$) one obtains the following expression for h:

$$h = \frac{2h_s K}{t}\left\{\sqrt{t} - K \ln\left[1 + \frac{\sqrt{t}}{K}\right]\right\} \quad (6)$$

where

$$K = \left\{\frac{k_e C_b \rho_b}{\pi h_s^2}\right\}^{1/2} \quad (7)$$

for an isothermal heat transfer surface and

$$K = \left\{\frac{\pi k_e C_b \rho_b}{4h_s^2}\right\}^{1/2} \quad (8)$$

for a constant heat flux boundary condition. The local wall-to-bed contact heat transfer coefficient is denoted by h.

The heat transfer model

Although, a comprehensive treatment of particle mixing and flow in the bulk and within the wall-to-blade clearance region of the vessel is given elsewhere [5, 9–12], a brief review of the pertinent results and observations is presented below.

The particle mixing mechanisms for beds of free-flowing particles and particles with reduced flowability (due to shape, surface roughness/stickiness, etc.) are different and can be characterized fairly well in terms of a parameter called the 'modified bulk compressibility' C [11]. The concept of 'C' is based on the inherent difference between the bulk densities of granular solids in packed and loose states. Loose state bulk density refers to the bulk weight when a given container is filled by pouring the granular material into it without any external compaction or vibration. Particles with $C \leqslant 0.08$ are free-flowing and particles with $C \geqslant 0.11$ exhibit reduced flowability. The bed to blade height ratio influences mixing of solids to a much greater extent than the blade speed.

Particle displacements and average velocities along the vessel cylindrical wall have been measured [12]. The experimental technique involved placing colored tracer particles along the wall and then noting their incremental change in position every blade pass (through the transparent end of the vessel). The conclusions are summarized in the following paragraph.

The free-flowing spherical particles ($C \leqslant 0.08$) move intermittently along the wall, i.e. they start to move as the blade approaches and come to a complete stop after its passage. A particle along the wall requires N_b number of passes of blade b1 (Fig. 1) to traverse the 'wetted' length of the vessel, if it were to stay along the wall. The 'wetted' length, L, denotes the circumferential length of the particle covered surface area as shown in Fig. 1. It should be noted that not all particles always traverse the whole length L. In

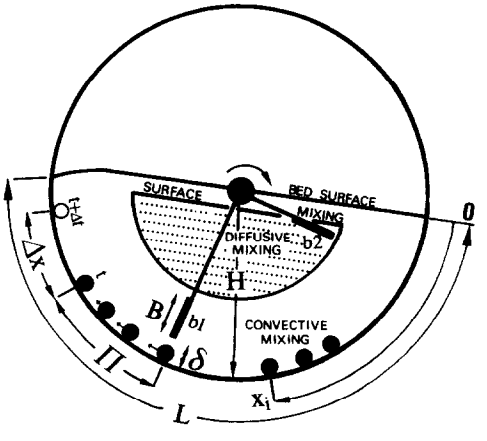

FIG. 1. Particle mixing mechanisms in a stirred granular bed.

fact, a significant fraction of them 'disappear' in the radial direction, i.e. there is continuous renewal of particles from the bulk. However, particles exhibiting reduced flowability (e.g. rice, linseed; $C \geqslant 0.11$) move as a 'plug' upstream of the blade (in the clearance region also) under some operating conditions, namely $\delta/d_p \leqslant 5$ and $\delta/d_p \leqslant 3$ for $D = 0.5$ and 0.25 m, respectively. Under such conditions, the particles in the clearance region are swept away by the blade in one pass leading to complete particle renewal along the entire length L.

In view of the aforementioned observations the wall-to-bed contact heat transfer model will be developed independently for free-flowing particles and particles moving in 'plug flow' upstream of the blade.

Case I: $N_b > 1$. The following treatment applies to cases where the particles along the wall move intermittently. Further, note that although movement was observed in all the particle layers within the clearance region, the discussion here is limited only to the layer adjacent to the wall. The implications of this limitation are discussed later. The above situation is depicted schematically in Fig. 2 assuming the blade to be stationary and the particles flowing past it.

Thus

$$V(x) = V_{bw} - V_{pi}(x) \tag{9}$$

where $V(x)$ is the instantaneous particle velocity relative to the blade in the region $0 \leqslant x \leqslant \Pi$. The upstream region of influence exerted along the wall by the blade is denoted by Π. It is defined as the distance between the moving blade and the particle upstream along the wall at the instant the particle starts to move (i.e. feels the influence of blade motion). The effects of different operating parameters are discussed in depth elsewhere [5, 12]. $V_{pi}(x)$ represents the local particle velocity along the wall in the stationary reference system (actual situation). Further, $V_{bw} = \omega D/2$, where ω is the angular velocity of blade rotation.

The following assumptions are employed in constructing the contact heat transfer model (Fig. 2).

(a) Contact heat transfer may be evaluated from the data on the particle layer adjacent to the heated surface.

(b) Particle renewal occurs from above and behind the moving blade at a uniform bulk temperature.

(c) Particles along the heated surface do not roll or tumble and their motion is governed entirely by the interaction of the force exerted by the moving blade and wall-to-particle friction.

(d) The bed porosity along the wall is constant and uniform in region Π.

(e) $V_{pi}(x) = 0$ for $x \to 0^-$ and $V_{pi}(x) = 0$ for $x \to \Pi^+$.

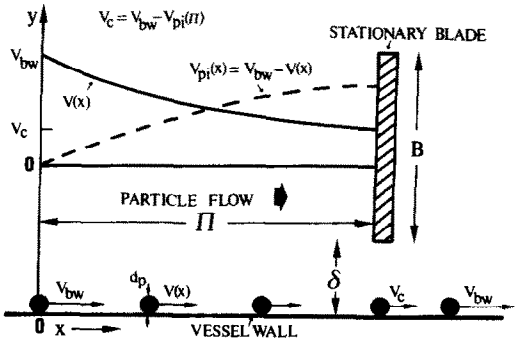

FIG. 2. Particle velocity profile at the wall for $N_b > 1$.

It was found that the thermal penetration depth [24] is less than half the size of the wall-to-blade clearance (i.e. $\delta/2$) under most operating conditions achieved in this study. This is due mainly to the low effective thermal diffusivity of the bed ($< 1 \times 10^{-6}$ m^2 s^{-1}). Also, the first 2–3 particle layers adjacent to the wall were observed to move at approximately the same velocity. Therefore, assuming no relative motion between the first 2–3 particle layers adjacent to the wall, the one-dimensional transient heat conduction equation can be employed with minimal error for $\delta/d_p \leqslant 5$. For $\delta/d_p > 5$, the particle–surface contact times increase considerably due to poor particle renewal rates. In such instances, the heat penetration depth exceeds several particle diameters. However, because particle movement within the clearance region for $\delta/d_p > 5$ is minimal for free-flowing spherical particles, the bed may be modelled as a homogeneous packed one within the thermal penetration depth. Therefore, employing equation (6) to evaluate h from the continuum 'packet renewal' model, based on the particle flow information adjacent to the wall, is expected to introduce minimal errors. Hence, assumption (a) is considered reasonable.

Assumption (b) is introduced on the basis of observed particle flow patterns [5, 11]. Assumption (c) discounts the fact that any particle rolling might alter the effective particle–surface contact time, by having the 'unheated' part of the particle contact the hot surface, as also discussed recently by Wang *et al.* [25]. Assumptions (d) and (e) are physically reasonable on the basis of visual observations.

Under the above-mentioned assumptions, the conservation of mass equation was employed [12] to evaluate the efficiency of particle renewal (η_0) as

$$\eta_0 = \frac{V_{pi}|_{x=\Pi}}{V_{bw}}. \tag{10}$$

The particle renewal efficiency was then related to particle flow dynamics [12] by considering a parabolic particle velocity profile within the region $0 \leqslant x \leqslant \Pi$. The choice of a parabolic particle velocity profile was based on earlier observations by the authors [5, 9]. The final results yielded the following implicit equation for η_0:

$$\eta_0 = 1 - \exp\left\{-\eta_0\left[1 + \left(1 + \frac{\Delta x}{\Pi}\right)\frac{\eta_0}{2}\right]\right\}. \tag{11}$$

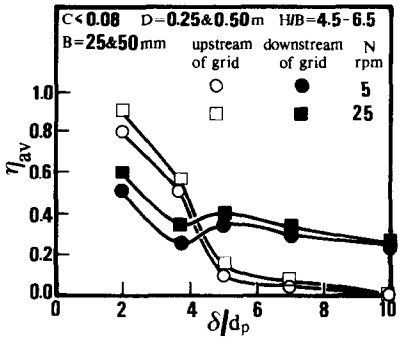

FIG. 3. Effect of δ/d_p on η_0.

Figure 3 presents the effect of wall-to-blade clearance size on particle renewal rates as evaluated from equation (11). The parameter, Δx, denotes the average particle displacement per blade pass at a given location along the wall. The data on Δx and Π were obtained from refs. [5, 12]. Figure 3 shows that while the average particle renewal efficiency upstream of the distributor grid drops sharply for $\delta/d_p > 2$, the corresponding drop is much less pronounced downstream of the grid. Therefore, increasing δ/d_p is expected to affect h_{av} adversely to a greater extent upstream, rather than downstream of the air distributor. The average particle renewal (η_{av}) rates along the whole length L were obtained by taking the arithmetic mean of the local particle renewal rates (η_0).

On the other hand, particle renewal rates are fairly constant over the entire heated length for beds of rice and linseed ($C \geqslant 0.11$) under circumstances where particle 'slippage' occurs in the clearance region. Such conditions are observed for $\delta/d_p > 3$ and $D = 0.25$ m. Also, the particle renewal rates are always higher for $C \geqslant 0.11$ as compared to those for particles with $C \leqslant 0.08$. In both cases however, η_{av} decreases with increased δ/d_p.

Estimation of contact time

The next step involves estimating the effective particle–surface contact time from the particle renewal rates. By definition a particle along the wall requires N_b blade passes to traverse length L. Let us assume that Δx and η_0 are constant over L. This simplified model is shown in Fig. 4. The probability of particle renewal in each zone of width Δx is denoted by η_0. This leads to a distribution of contact times with some particles staying longer at the wall than others. For example, the probability of a particle getting renewed in the very first zone is η_0, while the probability of a particle staying in contact with the entire length L is given by $(1-\eta_0)^{N_b}$. The contact time for the former particle is Δt while for the latter one it is $N_b \cdot \Delta t$. The time interval between two successive blade passes is denoted by Δt.

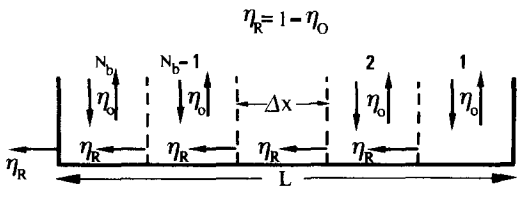

FIG. 4. Particle renewal model for $N_b > 1$.

The classical theory of probability (e.g. ref. [26]) can now be employed to determine the distribution of the particle–surface contact times. The model depicted in Fig. 4 consists of a sequence of N_b independent Bernoulli random trials. A Bernoulli random trial is defined as a trial consisting of only two outcomes (particle gets renewed or not). Thus, the probability of obtaining values of $j\eta_0$ and $(N_b-j)\eta_R$ in a specific sequence is

$$p(j) = \eta_0^j \eta_R^{N_b-j} = \eta_0^j (1-\eta_0)^{N_b-j}. \quad (12)$$

The number of distinct permutations of $j\eta_0$ and $(N_b-j)\eta_R$ is given by

$${}^{N_b}_{j}\mathscr{P} = \frac{N_b!}{j!(N_b-j)!}. \quad (13)$$

Equations (12) and (13) can be expressed in terms of the binomial probability function $f(j)$ as

$$f(j) = {}^{N_b}_{j}\mathscr{P}\eta_0^j(1-\eta_0)^{N_b-j}$$

$$j = 0, 1, \ldots, N_b, \; 0 \leqslant \eta_0 \leqslant 1. \quad (14)$$

The binomial probability distribution is a discrete probability distribution with two parameters, η_0 and N_b. Assigning specific values to η_0 and N_b identifies one binomial probability distribution from a family of all such distributions. Note that

$$\sum_{j=0}^{N_b} f(j) = 1.$$

The fraction of particles over length L with a contact time $(j+1)\cdot\Delta t$ can therefore be denoted by

$$f(N_b-j) = {}^{N_b}_{N_b-j}\mathscr{P}\eta_0^{N_b-j}\eta_R^j. \quad (15)$$

Also

$${}^{N_b}_{N_b-j}\mathscr{P} = {}^{N_b}_{j}\mathscr{P}.$$

The 'expected' value of the particle–surface contact time with the probability function $f(j)$ can therefore be expressed as [26]

$$E(t) = \sum_{j=0}^{N_b-1} {}^{N_b}_{j}\mathscr{P}\eta_0^{N_b-j}(1-\eta_0)^j(j+1)$$

$$+ N_b(1-\eta_0)^{N_b} \quad (16)$$

where $E(t)$ denotes the 'expected value' for contact time. The average particle–surface contact time over L is then simply evaluated as

$$t_{av} = E(t)\Delta t. \quad (17)$$

Note that the above equation consists of only two unknown parameters: N_b and η_0. The average contact time for a given operating condition can therefore be

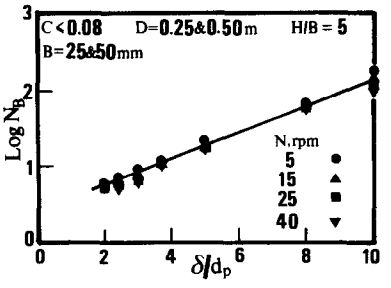

FIG. 5. Effect of δ/d_p on N_B.

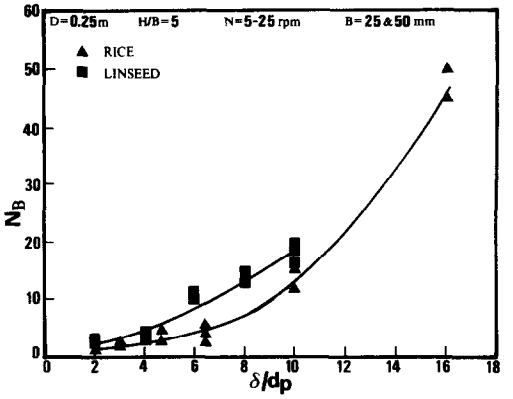

FIG. 6. Effect of δ/d_p on N_B.

evaluated solely from the particle flow information [5, 11, 12]. Equation (6) may then be employed along with equation (17) to evaluate h_{av}.

It can be seen from equation (17) that

$$t_{av} = \Delta t \quad \text{for} \quad \eta_0 = 1 \tag{18}$$

$$t_{av} = N_b \cdot \Delta t \quad \text{for} \quad \eta_0 = 0. \tag{19}$$

Equation (18) refers to the case of complete particle renewal per blade pass along the entire heated length L and may be used to obtain the upper bound for h_{av}. The lower bound for h_{av} can be evaluated using equation (19); it refers to the case where each particle stays in contact with the entire heated length L and the granular bed behaves like an intermittently moving packed bed. It should, however, be noted that a decrease in η_0 is usually accompanied by an increase in N_b. This is discussed below. Therefore, although the upper bound for h_{av} depends upon Δt only, the lower bound is a strong function of the operating parameters.

The information on N_b is important in estimating the average particle–surface contact time. Although discussed in depth elsewhere [5], some key results regarding the total number of blade passes required by a particle, if it were to traverse the whole length L, are reproduced here.

Figure 5 shows that for free-flowing spherical particles, the logarithm of N_B varies linearly with δ/d_p. N_B refers to the number of blade passes required by a particle to travel the distance from $0.1L$ to L, i.e. excluding the region $x/L < 0.1$. The particle motion in the region $x/L < 0.1$ was observed to be erratic and hence neglected in any analyses. Further, since Δx and Π both tend to zero for $x/L < 0.1$, $\eta_0 \to 1$ (equation (11)). Therefore, neglecting particle motion in this region is expected to introduce minimal errors in predicting h_{av}. N_B may be substituted for N_b in equation (16) for evaluating $E(t)$.

Figure 5 shows that the effect of agitator speed becomes important with increasing δ/d_p ratio. N_B decreases with increasing N. However, because of the high values of N_B (> 50) at large wall-to-blade clearances ($\delta/d_p \geqslant 5$), a reduction in N_B due to increasing blade rotational speed is expected to effect h_{av} only marginally. Therefore, for all practical purposes, the data in Fig. 5 can be represented by a single equation as

$$\log (N_B) = 0.16 \frac{\delta}{d_p} + 0.33. \tag{20}$$

An increase in C ($C \geqslant 0.11$) decreases N_B considerably. This can be seen by comparing the data for beds of rice and linseed in Fig. 6 with those for glass beads and millet in Fig. 5. Although, N_B increases with increasing δ/d_p for all particles, the increase is more pronounced for free-flowing spherical particles. Therefore, an increase in the δ/d_p ratio is expected to affect h_{av} adversely to a greater extent for free-flowing spherical particles as compared to ones with $C \geqslant 0.11$. This is verified to be true and is discussed in a concurrent publication [27].

Figure 7 displays the effect of δ/d_p ratio on the expected value $E(t)$ (equation (16)), simulated for a bed of spherical free-flowing particles in a 0.25 m diameter vessel heated along the entire particle covered surface area. Beyond $\delta/d_p = 3$, $E(t)$ rises dramatically. A 67% increase in δ/d_p ratio increases $E(t)$ by about 300%. This is expected to affect h_{av} adversely. Also $E(t)$ decreases by 38% on increasing N from 5 to 40 rev min^{-1} for $\delta/d_p = 5$. For $\delta/d_p \leqslant 3$, $E(t)$ is almost independent of N. It is noteworthy that the contact heat transfer model developed above is able to reproduce the experimental results of similar studies [22, 23] within $\pm 25\%$ for $\delta/d_p > 2.5$ for beds of free-flowing glass beads.

For vessels operating in the 'through-air flow'

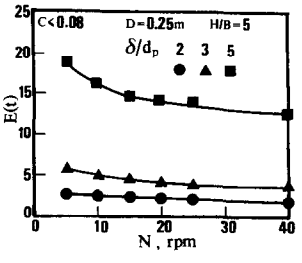

FIG. 7. Effect of δ/d_p on $E(t)$.

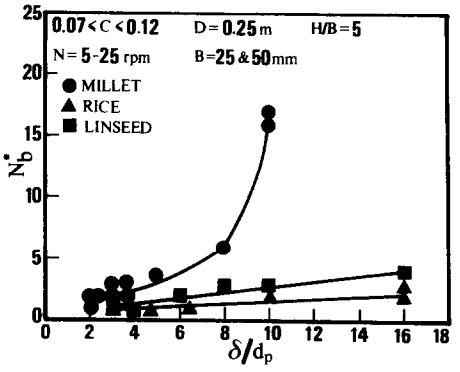

FIG. 8. Effect of δ/d_p on N_b^*.

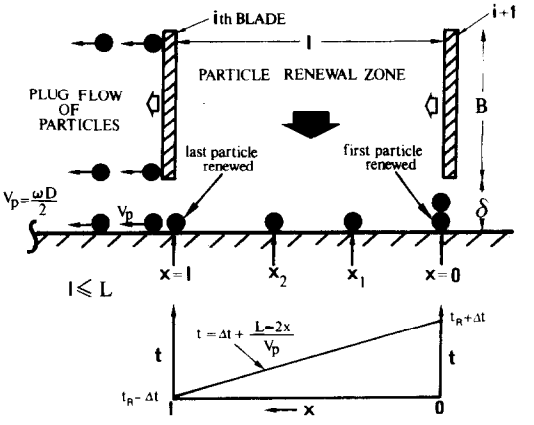

FIG. 9. Particle renewal mechanism for $N_b = 1$.

mode, the particle displacements along the wall were also recorded both before and after the distributor grid. Since, particles over the grid are essentially 'renewed' when exposed to the cooler inlet air, the overall wall-to-bed heat transfer problem can be divided into two independent sections—upstream and downstream of the air distributor grid. Figure 8 presents N_b^* vs δ/d_p data for downstream of the grid (in the positive x-direction). Note that in this case N_b^* is the number of blade passes required to travel the entire heated length following the grid. It was observed that a particle spends approximately equal periods of time upstream of and over the grid for $D = 0.25$ m and $H/B = 5$.

Another remark concerning equation (16) deserves attention. The equation can be modified to obtain local variations in the heat transfer coefficients over the length L by subdividing it into a number of 'sufficiently large' segments (a segment cannot be smaller than Δx at that given location). For such cases, equation (16) has to be subdivided into two parts—one to estimate the expected value for the particles getting renewed in a given segment and another for evaluating $E(t)$ for the particles not getting renewed and moving into the next segment. Since the variation of η_0 and N_b with x/L is known, the above analysis could in principle estimate the local heat transfer coefficients. However, such a rigorous analysis was not attempted and for practical engineering purposes equation (16) is expected to lead to reasonably accurate estimates of h_{av}.

Case II: $N_b = 1$. The following analysis is confined to the range of operating parameters that yield a 'plug flow' of the particles upstream of the moving blade and within the clearance. Thus the evaluation of the contact heat transfer simplifies to one in which the particles along the heated surface length L are renewed every blade pass. This is depicted schematically in Fig. 9. In order for equation (6) to be applicable, it is implicitly assumed that all the particles are renewed at a uniform temperature.

Figure 9 shows particles upstream of the ith blade at $x = l$ moving as a plug. Particle renewal occurs behind the ith blade as it moves through the region $0 \leqslant x \leqslant l$. The distance along the wall between two adjacent blades, i and $i+1$, is denoted by l. After renewal each particle rests for a certain period of time on the heated surface, before all particles upstream of the $(i+1)$th blade start to move again. This leads to a distribution of contact time in the region $0 \leqslant x \leqslant l$. For example, a freshly renewed particle at $x = x_1$ contacts the heated surface earlier than the one at $x = x_2$ and has to additionally traverse a greater distance along the wall once the bulk starts to move.

The contact time distribution as shown in Fig. 9 may be expressed as

$$t = \Delta t + \frac{L-2x}{V_p} \quad 0 \leqslant x \leqslant l. \tag{21}$$

The linear velocity of the particles along the wall is denoted by V_p. The overall average heat transfer coefficient (h_{av}) along L, is then evaluated as

$$h_{av} = \frac{\int_0^l \int_{x=0}^{x=l} (h\,dt)\,dx}{\int_0^L \int_{x=0}^{x=l} (dt)\,dx}. \tag{22}$$

The above equation transforms to

$$h_{av} = \frac{\int_{t_R-\Delta t}^{t_R+\Delta t} h\,dt}{\int_{t_R-\Delta t}^{t_R+\Delta t} dt} \cdot \frac{l}{L} \tag{23}$$

where

$$t_R = \frac{L}{V_p}; \quad \Delta t = \frac{l}{V_p}. \tag{24}$$

Finally

$$h_{av} = \frac{l}{2L\Delta t} \int_{t_R-\Delta t}^{t_R+\Delta t} h\,dt \quad n > \frac{\pi D}{L}. \tag{25}$$

Equation (6) may be employed to evaluate h. Equa-

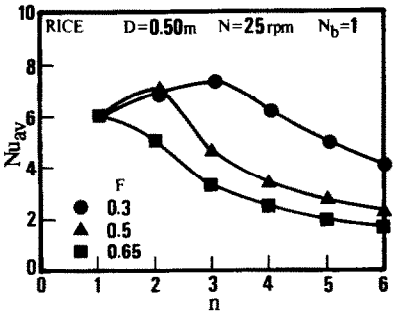

FIG. 10. Effect of n on Nu_{av} for $N_b = 1$.

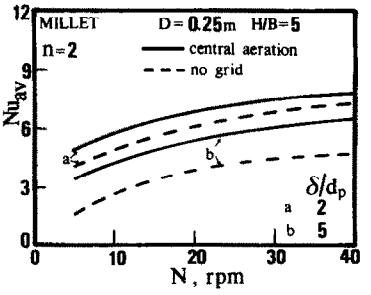

FIG. 11. Effect of centrally aerated grid on Nu_{av}.

tion (25) is valid for situations where more than one blade is immersed at any instant within the granular bed. Note, that although an increase in the number of blades (n) leads to a reduction in Δt, it may not necessarily enhance h_{av} due to a corresponding decrease in the fraction of freshly renewed particles, i.e. a decrease in the $1/L$ ratio. This effect is illustrated later.

For the case where only one blade is immersed in the bed at any given instant, equation (25) modifies to

$$h_{av} = \frac{1}{2t_R}\int_{\Delta t - t_R}^{\Delta t - t_R} h\,dt \quad n \leqslant \frac{\pi D}{L}. \tag{26}$$

For this case, particle renewal takes place along the whole length L.

The average particle–surface contact time (t_{av}) may also be evaluated from equation (21) for the above cases

$$t_{av} = t_R \quad n > \frac{\pi D}{L} \tag{27}$$

$$t_{av} = \Delta t \quad n \leqslant \frac{\pi D}{L}. \tag{28}$$

Equations (28) and (6) can also be employed to evaluate h_{av} with negligible error. Also, t_{av} evaluated from equation (17) with $N_b = 1$ and $\eta_0 = 1$ accurately predicts h_{av} for the above case. However, a significant error is introduced in evaluation of h_{av} for $n > \pi D/L$ when using equation (17) or equation (27) in conjunction with equation (6), if the corresponding decrease in particle renewal area is not included. Therefore, equations (25) and (26) are recommended for estimating h_{av} for the range of operating parameters that yield a 'plug flow' of particles.

Figure 10 presents results of a typical simulation on the effect of blade number (n) on the average Nusselt number Nu_{av}, for a bed of rice particles with $N_b = 1$. Contrary to intuition, an increase in n beyond a critical value adversely affects the average contact heat transfer rates. This is evident from equation (25) showing a reduction in the particle renewal surface area when more than one blade is immersed in the bed. Therefore, for beds of low hold-ups (e.g. $F = 0.3$), Nu_{av} increases up to $n = 3$, whereas, for deeper beds ($F \geqslant 0.65$), any increase in n beyond one diminishes Nu_{av}.

An increase in the number of blades, however, enhances Nu_{av} for beds with free-flowing particles ($N_b > 2$) by effectively reducing Δt. It should be noted that Fig. 9 depicts an ideal situation for $N_b = 1$ and in reality some, although little, particle renewal occurs along the whole heated length L in the wake of the moving blade when more than one blade is immersed in the bed. This phenomenon was noted visually; it is expected to attenuate the adverse effect of increasing n on Nu_{av}. Nevertheless, an increase in n does not enhance the contact heat transfer rates for deeper beds with $N_b = 1$, if it leads to having more than one blade being immersed within the bed at any instant.

Effect of aeration

As mentioned earlier, for centrally aerated granular beds the average contact heat transfer coefficient may be evaluated by considering the heated sections—upstream and downstream of the grid independently of each other. The particles in contact with the inlet air can be assumed to be at the uniform temperature of the rest of the bed. However, for granular solids stirred in vessels heated along the entire particle covered surface area (i.e. no grid), h_{av} would have to be evaluated by using N_B as shown in Figs. 5 and 6 and η_{av} over the entire heated length.

Figure 11 shows the effect of the air distributor grid (in the presence of aeration) on h_{av}. Aeration 'cools' the particles coming from the heated section upstream of the grid (i.e. from the direction opposite to the blade motion). The 'effective' lowering of t_{av} for centrally aerated beds leads to higher values of h_{av} as compared to gridless vessels. In order to have an unbiased comparison, the effect of air flow in increasing the bed thermal conductivity is not included in the simulation. Due to their plug flow motion, the effect of aeration on h_{av} is negligible for beds of rice and linseed ($\delta/d_p \leqslant 5$).

Note that although aeration enhances h_{av}, it causes a reduction in the total heat transfer surface area. For example, in the smaller vessel, the presence of the distributor grid decreases the available heated surface area by 25% for $H/B = 5$. On the other hand, the expected enhancement in h_{av} due to aeration, varies

between 20% ($N = 5$ rev min^{-1}) and 7% ($N = 40$ rev min^{-1}) for $\delta/d_p = 2$. The corresponding figures for $\delta/d_p = 5$ are 12 and 36%, respectively. Therefore, in order to maximize the total amount of heat transferred, it is advantageous to operate with centrally aerated beds, particularly if the operating conditions limit the minimum size of the wall-to-blade clearance. Also, as discussed by the authors [27], aeration helps promote thermal mixing within the granular bed leading to higher rates of contact heat transfer. This coupled with slightly enhanced h_{av} values, make through-air flow stirred vessels as the ideal choice (as compared to non-aerated ones) for heat/mass transfer processing of granular solids.

Air flow increases the effective bed thermal conductivity (k_e). The effect of aeration on k_e may be estimated by the correlation proposed by Wakao and Kaguei [28]. Several correlations are available [14, 28, 29] to evaluate the effective thermal conductivity of non-aerated packed granular beds from the knowledge of particle thermal conductivity and bed porosity. The effect of aeration on h_{av} through enhanced k_e is, however, marginal under the current operating conditions and low Fourier numbers. A similar observation has been reported by Ohmori *et al.* [30]. They found h_{av} to be almost independent of air flow rate (below minimum fluidization velocity) for thermally well-mixed beds of millet, rice and acrylic resin.

CONCLUSIONS

The following conclusions emerge from the wall-to-bed contact heat transfer model developed in this paper.

(1) The wall-to-bed contact heat transfer coefficient can be evaluated wholly from information on particle flow along the wall in the clearance region over the entire range of operating parameters examined in this study.

(2) A reduction in the wall-to-blade clearance size and/or an increase in the agitator rotational speed is expected to enhance contact heat transfer coefficients over the range of parameters under study. An increase in δ/d_p ratio is expected to adversely affect h_{av} to a greater extent for beds of free-flowing spherical particles as compared to those with reduced flowability.

(3) Centrally aerated stirred granular beds may be thermally more efficient than non-aerated ones, for large wall-to-blade clearance sizes.

Acknowledgements—The authors acknowledge Professor M. Okazaki, Dr H. Imakoma and M. Miyahara of Kyoto University, Japan, for their participation in the discussions on the above subject.

REFERENCES

1. K. Malhotra and A. S. Mujumdar, Immersed surface heat transfer in vibrated fluidized beds, *I&EC Res.* **26**, 1983–1992 (1987).
2. W. L. Root, Indirect drying of solids, *Chem. Engng* May 2, 52–64 (1983).
3. P. Y. McCormick, The key to drying solids, *Chem. Engng* Aug. 15, 113–122 (1988).
4. K. Ohashi, Effects of air through-flow on performance of indirect-heat agitated dryer, *Proc. 3rd Int. Drying Symp.*, pp. 467–473 (1982).
5. K. Malhotra, Particle flow and contact heat transfer characteristics of stirred granular beds, Ph.D. Thesis, McGill University, Montreal, Canada (1989).
6. J. Lehmberg, M. Hehl and K. Schugerl, Transverse mixing and heat transfer in horizontal rotary drum reactors, *Pow. Technol.* **18**, 149–163 (1977).
7. G. W. J. Wes, A. A. H. Drinkenburg and S. Stemerding, Solids mixing and residence time distribution in a horizontal rotary drum reactor, *Pow. Technol.* **13**, 177–184 (1976).
8. E. U. Schlunder, Vacuum contact drying of free flowing mechanically agitated particulate material, *DRYING '85* (Edited by R. Toei and A. S. Mujumdar), pp. 75–83. Hemisphere/Springer, New York (1985).
9. K. Malhotra, H. Imakoma, A. S. Mujumdar and M. Okazaki, Fundamental particle mixing studies in an agitated bed of granular materials in a cylindrical dryer, *Pow. Technol.* **55**, 107–114 (1988).
10. K. Malhotra, A. S. Mujumdar and M. Okazaki, Particle flow patterns in a mechanically stirred two-dimensional cylindrical vessel, *Pow. Technol.* **60**, 179–189 (1990).
11. K. Malhotra and A. S. Mujumdar, Particle mixing and solids flowability in granular beds stirred by paddle-type blades, *Pow. Technol.* **61**(2), 155–164 (1990).
12. K. Malhotra, M. Miyahara and A. S. Mujumdar, Estimation of particle renewal rates along the wall in a mechanically stirred granular bed, *Chem. Engng Process.* **27**(3), 121–130 (1990).
13. N. I. Gelperin and V. G. Einstein, Heat transfer in fluidized beds. In *Fluidization* (Edited by J. F. Harrison and D. Davidson), Chap. 10. Academic Press, New York (1971).
14. E. U. Schlunder, *Particle Heat Transfer, Proc. 7th Int. Heat Transfer Conf.* (Edited by U. Grigull, E. Hahne, K. Stephan and J. Straub), pp. 184–193. Hemisphere, New York (1982).
15. J. S. M. Botterill and M. Desai, Limiting factors in gas-fluidized bed heat transfer, *Pow. Technol.* **6**, 231–238 (1972).
16. W. N. Sullivan and R. H. Sabersky, Heat transfer to flowing granular media, *Int. J. Heat Mass Transfer* **18**, 97–107 (1975).
17. D. Gloski, L. Glicksman and N. Decker, Thermal resistance at a surface in contact with fluidized bed particles, *Int. J. Heat Mass Transfer* **27**, 599–610 (1984).
18. P. Lybaert, Contribution à l'étude du transfert de chaleur entre un matériau particulaire et la paroi dans les échangeurs rotatifs indirects, Ph.D. Thesis, Faculté Polytechnique de Mons, Belgium (1984).
19. K. Malhotra and A. S. Mujumdar, Effect of particle shape on the particle–surface thermal contact resistance, *J. Chem. Engng Japan* **23**(4), 509–512 (1990).
20. H. S. Mickley and D. F. Fairbanks, Mechanism of heat transfer in fluidized beds, *A.I.Ch.E. Jl* **1**, 374–384 (1955).
21. H. Martin, Heat and mass transfer in fluidized beds, *Int. Chem. Engng* **22**(1), 30–43 (1982).
22. T. Ohmori, Heat transfer in indirect-heat agitated dryer, Ph.D. Thesis, Kyoto University, Kyoto, Japan (1984).
23. R. Toei, T. Ohmori, T. Furuta and M. Okazaki, *Heat Transfer Coefficient between Heating Wall and Agitated Granular Bed, DRYING '85* (Edited by R. Toei and A. S. Mujumdar), pp. 209–214. Hemisphere/Springer, New York (1985).
24. H. S. Carslaw and J. C. Jaeger, *Conduction of Heat in Solids*. Oxford University Press, Oxford (1959).

25. D. G. Wang, S. S. Sadhal and C. S. Campbell, Particle rotation as a heat transfer mechanism, *Int. J. Heat Mass Transfer* **32**, 1413–1423 (1989).
26. J. Neter, W. Wasserman and G. A. Whitmore, *Applied Statistics*. Allyn & Bacon, Toronto (1979).
27. K. Malhotra and A. S. Mujumdar, Wall-to-bed contact heat transfer rates in mechanically stirred granular beds, *Int. J. Heat Mass Transfer* **34**, 427–435 (1991).
28. N. Wakao and S. Kaguei, *Heat and Mass Transfer in Packed Beds*. Gordon & Breach, New York (1982).
29. S. Yagi and D. Kunii, Studies on effective thermal conductivities in packed beds, *A.I.Ch.E. Jl* **3**(3), 373–381 (1957).
30. T. Ohmori, M. Miyahara, M. Okazaki and R. Toei, Heat transfer from a submerged tube moving in a granular bed, *J. Chem. Engng Japan* **21**(2), 141–147 (1988).

MODELE DU TRANSFERT THERMIQUE PAR CONTACT DANS DES LITS GRANULAIRES BRASSES MECANIQUEMENT

Résumé—Bien que largement exploitée dans l'industrie, la conception de lits brassés mécaniquement est encore un art. Cette recherche, probablement pour la première fois, essaie d'évaluer les flux thermiques dans le contact surface-lit pour des lits remués par des lames, à partir de la connaissance fondamentale des caractéristiques de l'écoulement des particules. On présente un modèle physique pour le coefficient de transfert thermique paroi-lit qui est basé sur le taux de renouvellement à la surface chaude. Les taux de renouvellement de particules sont estimés à partir des informations expérimentales sur le mouvement particulaire au voisinage de la paroi chaude dans une configuration bidimensionnelle. Le modèle de transfert thermique inclut les effets de la vitesse de rotation de l'agitateur, de la taille du jeu entre paroi et lame, de l'aération des solides.

MODELL FÜR DEN KONTAKTWÄRMETRANSPORT IN EINER MECHANISCH BEWEGTEN SCHÜTTUNG

Zusammenfassung—Obwohl sie im industriellen Bereich vielfach verwendet werden, ist die Konstruktion mechanisch gerührter Heizkessel noch immer eine Kunst. In der vorliegenden Arbeit wird versucht—vielleicht zum ersten Mal—die Wärmeübertragung durch Kontakt zwischen Oberfläche und geschüttetem Bett zu berechnen, und zwar für spezielle Schüttungen, die mechanisch durch Schaufeln bewegt werden. Es wird ein physikalisches Modell vorgestellt für den Kontakt-Wärmeübergangskoeffizienten von der Wand an die Schüttung. Das Modell beruht auf der "Erneuerungs"-Geschwindigkeit der Partikel an der beheizten Oberfläche. Diese Erneuerungs-Geschwindigkeit der Partikel wird ausschließlich aus Meßdaten über die Partikelbewegung in der Nähe der beheizten Kesselwand in einer zweidimensionalen Anordnung bestimmt. Das Modell für die Wärmeübertragung berücksichtigt die Einflüsse der Drehgeschwindigkeit des Rührers, des Abstandes zwischen Wand und Schaufel, des Fließvermögens der Feststoffpartikel sowie der Auflockerung.

МОДЕЛЬ КОНТАКТНОГО ТЕПЛОПЕРЕНОСА В МЕХАНИЧЕСКИ ПЕРЕМЕШИВАЕМЫХ ГРАНУЛИРОВАННЫХ СЛОЯХ

Аннотация—Несмотря на широкое применение в промышленности, разработка нагревательных камер с механически перемешиваемыми слоями еще далека до своего завершения. В настоящем исследовании делается попытка, возможно, впервые, оценить интенсивность теплопереноса при контакте слоя с поверхностью для частиц, перемешиваемых лопаточным устройством, на основе знаний характеристик потока частиц. Представлена физическая модель контактного теплопереноса между стенкой и слоем, основанная на скорости смены частиц у нагреваемой поверхности. Скорости смены частиц оцениваются исключительно по измерениям движения частиц вблизи нагреваемой стенки камеры двумерной конфигурации. Модель теплопереноса учитывает влияние скорости вращения мешалки, зазора между стенкой и лопастаями, а также текучесть и продуваемость твердых частиц.